# Breathers in $\mathcal{PT}$-symmetric optical couplers

I. V. Barashenkov,[1,2,3] Sergey V. Suchkov,[1,4] Andrey A. Sukhorukov,[1] Sergey V. Dmitriev,[4] and Yuri S. Kivshar[1]

[1]*Nonlinear Physics Centre, Research School of Physics and Engineering, Australian National University, Canberra,*
*Australian Capital Territory 0200, Australia*
[2]*Department of Mathematics, University of Cape Town, Rondebosch 7701, South Africa*
[3]*Joint Institute for Nuclear Research, Dubna, Russia*
[4]*Institute for Metal Superplasticity Problems, Russian Academy of Sciences, Ufa 450001, Russia*

We show that parity-time- ($\mathcal{PT}$-) symmetric coupled optical waveguides with gain and loss support localized oscillatory structures similar to the breathers of the classical $\phi^4$ model. The power carried by the $\mathcal{PT}$ breather oscillates periodically, switching back and forth between the waveguides, so that the gain and loss are compensated on the average. The breathers are found to coexist with solitons and to be prevalent in the products of the soliton collisions. We demonstrate that the evolution of a small-amplitude breather's envelope is governed by a system of two coupled nonlinear Schrödinger equations and employ this Hamiltonian system to show that small-amplitude $\mathcal{PT}$ breathers are stable.

PACS number(s): 42.65.Tg, 42.25.Bs, 11.30.Er, 42.82.Et

## I. INTRODUCTION

Light propagation in parity-time- ($\mathcal{PT}$-) symmetric optical systems with balanced gain and loss has been under intense scrutiny in the past few years. The concept has its roots in quantum mechanics where a $\mathcal{PT}$-symmetric non-Hermitian Hamiltonian may have an entirely real spectrum of eigenvalues [1,2]. In optics, the $\mathcal{PT}$ symmetry can be achieved by an appropriate modulation of the complex refractive index [3–5].

The symmetric optical systems should display a variety of unusual and often counterintuitive phenomena including an unconventional beam refraction [6,7], Bragg scattering [8,9], nonreciprocal Bloch oscillations [10], symmetry-breaking transitions [11,12], a loss-induced optical transparency [13], conical diffraction [14], an additional type of Fano resonance [15], chaos [16], and nonlocality manifested in the nontrivial effect of the boundaries [17]. Recently, optical $\mathcal{PT}$-symmetric couplers [12,13] and lattices [18] have been realized experimentally.

Nonlinear effects in $\mathcal{PT}$-symmetric systems are of particular interest for both fundamental and applied science. They offer the potential for an efficient control of light, including all-optical low-threshold switching [19–21] and unidirectional invisibility [20]. In addition, nonlinearity can compensate the diffraction of stationary light beams and dispersion of light pulses, allowing the formation of spatial and temporal solitons.

There has already been a large number of studies of optical solitons in $\mathcal{PT}$-symmetric systems. Solitons in complex one-dimensional potentials have been analyzed on the basis of the nonlinear Schrödinger equation [22–32]. Two-dimensional symmetric potentials were dealt with in Refs. [26,29,33]. The authors of [34–37] classified solitons in planar $\mathcal{PT}$-symmetric couplers, whose geometry is intermediate between one- and two-dimensional lattices.

The $\mathcal{PT}$-symmetric solitons considered in the above publications represented stationary self-localized modes. The solitons arise due to the exact compensation of the gain and loss at each moment of time. A more general type of localized objects was identified in [37], where the unstable solitons were observed to seed spatially localized temporally

periodic states. (In the context of planar stationary waveguides, these are interpreted as transversally localized structures with profiles oscillating along the waveguide.) These objects resemble breathers in conservative systems (such as the $\phi^4$ and sine-Gordon equations) [38]; hence they were referred to simply as *breathers* [37].

In this paper the $\mathcal{PT}$ breathers are studied in more detail. First, we derive the amplitude equations for oscillatory solutions in a planar $\mathcal{PT}$-symmetric nonlinear optical coupler (the equations for the envelopes of the oscillatory wave packets). The amplitude equations turn out to be Hamiltonian—despite the fact that the original system includes both gain and loss. These Hamiltonian equations are then used to show that the (zero-velocity) $\mathcal{PT}$ breathers form two-parameter families with variable amplitude, localization width, and contrast of power density oscillations. We also employ these equations to establish the stability of the breathers with small amplitude. Finally, the planar $\mathcal{PT}$-symmetric coupler is simulated numerically. The results of our numerical simulations demonstrate that the breathers are generic objects which are commonly formed as a result of soliton collisions.

The outline of the paper is as follows. In Sec. II, we introduce the mathematical model, and in the subsequent section, derive equations for the slowly varying envelopes of its oscillatory solutions. Section IV uses these amplitude equations to classify the $\mathcal{PT}$-symmetric breather states. The stability of the small-amplitude breathers is established in Sec. V. In the next Section (Sec. VI), we describe the formation of breathers in soliton-soliton collisions. Finally, Sec. VII summarizes the results of this study.

## II. MODEL

The $\mathcal{PT}$-symmetric coupler, i.e., a pair of coupled waveguides with power gain in one waveguide and optical loss of equal rate in the other, has been studied theoretically [4,5,20,21,39] and experimentally [12,13]. Optical systems that include the $\mathcal{PT}$-symmetric coupler as a structural element [15,17,40] and systems consisting of arrays of such
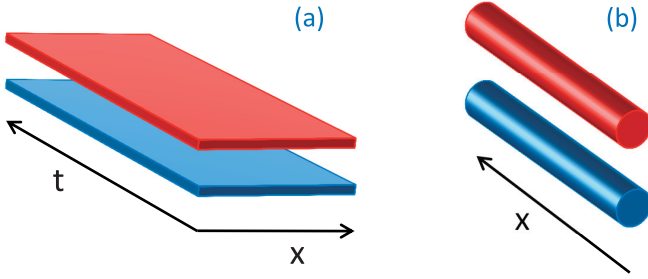
FIG. 1. (Color online) A schematic representation of $\mathcal{PT}$-symmetric coupled waveguides with gain (red, top) and loss (blue, bottom, waveguide). (a) Two planar waveguides carrying stationary light beams. Here $t$ and $x$ indicate the longitudinal and transverse spatial coordinates, respectively. (b) A pair of one-dimensional waveguides where light pulses undergo temporal evolution as they travel along the $x$ axis.

couplers [7,14,23,34,39,41,42] have also been discussed in the literature.

Following [35,37] we analyze the diffraction of optical beams propagating in a *planar* $\mathcal{PT}$ coupler, in media with Kerr-type nonlinearity. The amplitudes of the active and passive modes in this setting satisfy a system of two coupled nonlinear Schrödinger equations,

$$iu_t + u_{xx} + 2|u|^2 u = -v + i\gamma u,$$
$$iv_t + v_{xx} + 2|v|^2 v = -u - i\gamma v. \tag{2.1}$$

Here $t$ is the (spatial) coordinate in the propagation direction and $x$ is the transverse coordinate. The coefficient $\gamma > 0$ is the amplification rate for the waveguide with gain and, at the same time, the damping rate for the waveguide with loss. This planar coupler is schematically shown in Fig. 1(a). It is fitting to note here that the system (2.1) emerges as the continuum limit of the chain of $\mathcal{PT}$ couplers considered in [34].

The same $\mathcal{PT}$-symmetric system (2.1) can describe the propagation of optical pulses (rather than stationary light beams) [37]. This alternative interpretation of Eqs. (2.1) arises if $t$ and $x$ stand for the time and distance in the frame of reference traveling along with the pulse. This is the arrangement illustrated by Fig. 1(b).

The system (2.1) is not conservative. Neither the individual powers associated with the two modes,

$$\mathcal{P}_u = \int |u|^2 dx, \quad \mathcal{P}_v = \int |v|^2 dx, \tag{2.2}$$

nor their sum are conserved. The total power satisfies

$$\frac{d}{dt}(\mathcal{P}_u + \mathcal{P}_v) = 2\gamma(\mathcal{P}_u - \mathcal{P}_v), \tag{2.3}$$

which implies that it remains constant only on solutions which have $\mathcal{P}_u = \mathcal{P}_v$ for all times [37].

## III. WEAKLY NONLINEAR AMPLITUDE EQUATIONS

We start our analysis by transforming Eqs. (2.1) to a system with a diagonal linear part. Assuming $\gamma < 1$ and defining

$$a = \frac{e^{i\theta}u - v}{2\omega_0}, \quad b = \frac{e^{-i\theta}u + v}{2\omega_0}, \tag{3.1}$$

where

$$\theta = \arcsin\gamma, \quad \omega_0 = \cos\theta,$$

Eqs. (2.1) become

$$ia_t + a_{xx} - \omega_0 a + 2(|a|^2 + 2|b|^2)a$$
$$+ 4ie^{-i\theta}\gamma a^2 b^* + 2e^{2i\theta}a^*b^2 = 0,$$
$$ib_t + b_{xx} + \omega_0 b + 2(2|a|^2 + |b|^2)b$$
$$- 4ie^{i\theta}\gamma a^*b^2 + 2e^{-2i\theta}a^2 b^* = 0. \tag{3.2}$$

The system (3.2) has two simple reductions or, equivalently, two invariant manifolds. Letting $b = 0$, Eqs. (3.2) reduce to a scalar nonlinear Schrödinger equation,

$$ia_t + a_{xx} - \omega_0 a + 2|a|^2 a = 0, \tag{3.3}$$

while letting $a = 0$ yields a scalar Schrödinger equation with the opposite sign of the frequency term:

$$ib_t + b_{xx} + \omega_0 b + 2|b|^2 b = 0. \tag{3.4}$$

Both (3.3) and (3.4) have soliton solutions and hence the system (3.2) admits two types of "simple" soliton: one with $b = 0$ and the other one with $a = 0$. These low- and high-frequency solitons have been analyzed before [34,35,37]. Here, our aim is to construct more general solutions with both components nonzero.

To this end, we note that when $a$ and $b$ are so small that the nonlinear part in (3.2) can be neglected, the resulting linear system has a family of spatially homogeneous stationary-wave solutions: $a = \mathcal{A}_0 e^{-i\omega_0 t}$, $b = \mathcal{B}_0 e^{i\omega_0 t}$. To search for the nonlinear counterparts of these, we consider a long-wavelength small-amplitude configuration:

$$a(x,t) = \epsilon^{1/2}A(X,t), \quad b(x,t) = \epsilon^{1/2}B(X,t), \tag{3.5}$$

where $X = \epsilon^{1/2}x$ and $\epsilon$ is a small parameter ($\epsilon > 0$). The $O(1)$ fields $A$ and $B$ satisfy

$$iA_t + \epsilon A_{XX} - \omega_0 A + 2\epsilon(|A|^2 + 2|B|^2)A$$
$$+ 4ie^{-i\theta}\epsilon\gamma A^2 B^* + 2e^{2i\theta}\epsilon A^*B^2 = 0,$$
$$iB_t + \epsilon B_{XX} + \omega_0 B + 2\epsilon(2|A|^2 + |B|^2)B$$
$$- 4ie^{i\theta}\epsilon\gamma A^*B^2 + 2e^{-2i\theta}\epsilon A^2 B^* = 0. \tag{3.6}$$

Solutions of the system (3.6) can be sought for as expansions in powers of $\epsilon$:

$$A = A_0 + \epsilon A_1 + \cdots, \quad B = B_0 + \epsilon B_1 + \cdots. \tag{3.7}$$

We also assume that the coefficients $A_n$ and $B_n$ depend on a hierarchy of "slow times" and "zoomed-out" spatial coordinates: $A_n = A_n(T_0, T_1, \ldots; X_0, X_1, \ldots)$, $B_n = B_n(T_0, T_1, \ldots; X_0, X_1, \ldots)$, where

$$T_n = \epsilon^n t, \quad X_n = \epsilon^n X, \quad n = 0, 1, 2, \ldots. \tag{3.8}$$

In the limit $\epsilon \to 0$ the scaled time and space variables decouple and can be treated as independent. In what follows, we adopt a shorthand notation,

$$D_n = \partial/\partial T_n, \quad \partial_n = \partial/\partial X_n.$$

Note that the parameter $\epsilon$ is not pegged to any scale of the original model (2.1),(3.2). Therefore we expect it to be

absorbable in the parameters of the solutions that we will end up with.

Substituting the expansions (3.7) in (3.6), we equate coefficients of like powers of $\epsilon$. The order $\epsilon^0$ gives

$$(i D_0 - \omega_0)A_0 = 0, \quad (i D_0 + \omega_0)B_0 = 0,$$

whence

$$A_0 = e^{-i\tau} p, \quad B_0 = e^{i\tau} q, \tag{3.9}$$

with

$$\tau = \omega_0 T_0.$$

The coefficients $p$ and $q$ are functions of all variables except $T_0$.

The order $\epsilon^1$ produces

$$
\begin{aligned}
(i D_0 - \omega_0)A_1 &= -\big[i D_1 A_0 + \partial_0^2 A_0 + 2(|A_0|^2 + 2|B_0|^2)A_0 \\
&\quad + 4i e^{-i\theta}\gamma A_0^2 B_0^* + 2e^{2i\theta} B_0^2 A_0^*\big], \\
(i D_0 + \omega_0)B_1 &= -\big[i D_1 B_0 + \partial_0^2 B_0 + 2(|B_0|^2 + 2|A_0|^2)B_0 \\
&\quad - 4i e^{i\theta}\gamma B_0^2 A_0^* + 2e^{-2i\theta} A_0^2 B_0^*\big].
\end{aligned}
\tag{3.10}
$$

To eliminate the secular terms, we impose

$$
\begin{aligned}
i D_1 p + \partial_0^2 p + 2(|p|^2 + 2|q|^2)p &= 0, \\
i D_1 q + \partial_0^2 q + 2(|q|^2 + 2|p|^2)q &= 0.
\end{aligned}
\tag{3.11}
$$

The remaining terms in the right-hand sides of (3.10) involve the third harmonics only; hence we get, for $A_1$ and $B_1$,

$$
\begin{aligned}
A_1 &= \frac{1}{2\omega_0}(e^{2i\theta} q^2 p^* e^{3i\tau} - 4i e^{-i\theta}\gamma p^2 q^* e^{-3i\tau}), \\
B_1 &= -\frac{1}{2\omega_0}(4i e^{i\theta}\gamma q^2 p^* e^{3i\tau} + e^{-2i\theta} p^2 q^* e^{-3i\tau}).
\end{aligned}
\tag{3.12}
$$

Proceeding to the order $\epsilon^2$, and setting the corresponding secular terms to zero, we obtain

$$
\begin{aligned}
i D_2 p + 2\partial_0 \partial_1 p + \frac{1}{\omega_0}(|q|^2 - 2|p|^2)|q|^2 p &= 0, \\
i D_2 q + 2\partial_0 \partial_1 q + \frac{1}{\omega_0}(2|q|^2 - |p|^2)|p|^2 q &= 0,
\end{aligned}
\tag{3.13}
$$

where we have substituted for $A_1$ and $B_1$ from (3.12).

According to Eqs. (3.11), the variations in the amplitudes $p$ and $q$ become noticeable only over long periods of time, $\Delta t \sim \epsilon^{-1}$. Equations (3.13) govern the evolution of these amplitudes over even longer time intervals, $\Delta t \sim \epsilon^{-2}$. It is convenient to combine Eqs. (3.11) and (3.13) into a system that takes care of the evolution on *both* slow scales. To this end, we add Eqs. (3.11) to Eqs. (3.13) multiplied by $\epsilon$ and define $T = \epsilon t$. Since the amplitudes do not depend on $T_0$, the chain rule gives $\partial/\partial T = D_1 + \epsilon D_2 + \epsilon^2 D_3 + \cdots$. Thus, to within $O(\epsilon^2)$, we have $D_1 p + \epsilon D_2 p = p_T$ and $D_1 q + \epsilon D_2 q = q_T$, and so the resulting pair of equations can be written as

$$
\begin{aligned}
i p_T + p_{XX} + 2(|p|^2 + 2|q|^2)p + \frac{\epsilon}{\omega_0}(|q|^2 - 2|p|^2)|q|^2 p &= 0, \\
i q_T + q_{XX} + 2(|q|^2 + 2|p|^2)q + \frac{\epsilon}{\omega_0}(2|q|^2 - |p|^2)|p|^2 q &= 0.
\end{aligned}
$$
$$\tag{3.14}$$

(Here $\epsilon \geqslant 0$.) This is a Hamiltonian system, with the Hamilton functional

$$
\begin{aligned}
H = \int \big[ &|p_X|^2 + |q_X|^2 - (|p|^4 + |q|^4 + 4|pq|^2) \\
&+ \epsilon \omega_0^{-1} |pq|^2 (|p|^2 - |q|^2)\big] dX.
\end{aligned}
$$

The amplitude equations (3.14) describe the evolution of the slowly changing envelope of a small-amplitude, weakly localized packet of waves with the carrier frequency $\omega_0$. Over time intervals $\epsilon^{-1} \lesssim \Delta t \lesssim \epsilon^{-2}$, Eqs. (3.14) are equivalent to the original system (2.1). This remarkable equivalence of a dissipative and conservative system, holding for a particular but fairly broad class of trajectories, is attributable to the $\mathcal{PT}$ symmetry of the former.

Setting $\epsilon = 0$, the system (3.14) becomes

$$
\begin{aligned}
i p_T + p_{XX} + 2(|p|^2 + 2|q|^2)p &= 0, \\
i q_T + q_{XX} + 2(|q|^2 + 2|p|^2)q &= 0.
\end{aligned}
\tag{3.15}
$$

This vector nonlinear Schrödinger equation has been extensively studied in the literature [43–55]. On the other hand, the system (3.14) with $\epsilon \neq 0$ does not seem to have been discussed before.

Note that both Eq. (3.14) and the "curtailed" system (3.15) govern the *small-amplitude* breathers only, with $u, v \sim \epsilon^{1/2}$. However Eq. (3.14) has an advantage over Eq. (3.15) in that the former system has a longer range of validity. While Eq. (3.15) ceases to be valid for times exceeding $\epsilon^{-1}$, Eq. (3.14) remains accurate for times as long as $\epsilon^{-2}$.

Our second reason behind the evaluation of the second-order corrections in the perturbation expansion was related to the conservative property of the amplitude equations (3.14) and (3.15). Once the first-order amplitude equations are found to be given by a Hamiltonian system [the system (3.11)], the question arises whether this property is specific to the first-order evolution only. The fact that the second-order dynamics is also governed by a Hamiltonian system [Eq. (3.14)] suggests then that the energy conservation is an inherent property of the small-amplitude oscillations. We conjecture that this property is valid to all orders in the perturbation theory (and may be violated only by terms that lie beyond all orders).

## IV. BREATHER SOLUTIONS

One simple solution of Eqs. (3.14) is

$$p = e^{i[\mu T + (V/2)X]}\sqrt{\mu}\, \mathrm{sech}[\sqrt{\mu}(X - VT)], \quad q = 0. \tag{4.1}$$

The other one is given by

$$p = 0, \quad q = e^{i[\nu T + (W/2)X]}\sqrt{\nu}\, \mathrm{sech}[\sqrt{\nu}(X - WT)]. \tag{4.2}$$

These two solutions of (3.14) will be referred to as *degenerate solitons*. The parameters $\mu > 0$, $\nu > 0$, $V$, and $W$ can be chosen arbitrarily. Here $\sqrt{\mu}$ and $\sqrt{\nu}$ give the amplitudes of the degenerate solitons, and $V$ and $W$ are their velocities.

The degenerate-soliton solutions of Eq. (3.14) correspond to the solitons of the scalar reductions (3.3) and (3.4) of the original system (2.1). The degenerate soliton (4.1) corresponds to the low-frequency soliton of (2.1), and the solution (4.2) to its high-frequency counterpart [34,35,37]. The vector of the power densities $\{|u|^2, |v|^2\}$ associated with

each of these solutions describes a pulse traveling, without oscillations, at the velocities $v = \epsilon^{1/2}V$ and $w = \epsilon^{1/2}W$, respectively.

Our main interest is in solutions of the system (3.14) which have both components nonzero. Thanks to the Galilian invariance of (3.14), it is sufficient to consider separable solutions corresponding to nonpropagating waves:

$$p = e^{i\mu T}P(X), \quad q = e^{i\nu T}Q(X). \quad (4.3)$$

The spatial parts $P$ and $Q$ satisfy

$$P'' - \mu P + 2(|P|^2 + 2|Q|^2)P + \frac{\epsilon}{\omega_0}(|Q|^4 - 2|PQ|^2)P = 0,$$

$$Q'' - \nu Q + 2(|Q|^2 + 2|P|^2)Q + \frac{\epsilon}{\omega_0}(2|PQ|^2 - |P|^4)Q = 0,$$
$$(4.4)$$

where the double prime indicates $d^2/dX^2$.

Localized solutions of the stationary equations (4.4) give rise to oscillatory, breatherlike, configurations in the original model (2.1):

$$u(x,t) = \epsilon^{1/2}[Qe^{i\omega_2 t} + Pe^{-i\omega_1 t}] + O(\epsilon^{3/2}),$$

$$v(x,t) = \epsilon^{1/2}[Qe^{i(\omega_2 t + \theta)} - Pe^{-i(\omega_1 t + \theta)}] + O(\epsilon^{3/2}),$$

where $P = P(\epsilon^{1/2}x)$, $Q = Q(\epsilon^{1/2}x)$, and

$$\omega_1 = \omega_0 - \epsilon\mu, \quad \omega_2 = \omega_0 + \epsilon\nu.$$

The corresponding $|u|^2$ and $|v|^2$ are

$$|u|^2 = \epsilon(|P|^2 + |Q|^2) + \epsilon[QP^* e^{i(\omega_1 + \omega_2)t} + \text{c.c.}],$$

$$|v|^2 = \epsilon(|P|^2 + |Q|^2) - \epsilon[QP^* e^{i(\omega_1 + \omega_2)t + 2i\theta} + \text{c.c.}],$$

where c.c. stands for the complex conjugate of the immediately preceding term and we neglected the $O(\epsilon^2)$ corrections. These quantities show temporal oscillations with the frequency $\omega_1 + \omega_2 = 2\cos\theta + \epsilon(\nu - \mu)$.

In this paper, we confine ourselves to the simplest choice of $\nu = \mu$. (A brief comment on a more general situation with $\nu \neq \mu$ is in Appendix A.) An additional simplification is attained by restricting consideration to real solutions. For real $P$ and $Q$ Eqs. (4.4) reduce to

$$P'' - \mu P + 2P^3 + 4Q^2 P + \frac{\epsilon}{\omega_0}(Q^2 - 2P^2)Q^2 P = 0,$$

$$Q'' - \mu Q + 2Q^3 + 4P^2 Q + \frac{\epsilon}{\omega_0}(2Q^2 - P^2)P^2 Q = 0.$$
$$(4.5)$$

When $\epsilon = 0$, the system (4.5) has an explicit solution

$$P_0(X) = Q_0(X) = \sqrt{\frac{\mu}{3}} \operatorname{sech}(\sqrt{\mu}X). \quad (4.6)$$

The terms proportional to $\epsilon$ in (4.5) are regular perturbations, i.e., the perturbed solution satisfying the boundary conditions $P(X), Q(X) \to 0$ as $|X| \to \infty$ exists for all sufficiently small $\epsilon$. To show this, we expand $P$ and $Q$ in powers of $\epsilon$,

$$P = P_0 + \epsilon P_1 + \epsilon^2 P_2 + \cdots, \quad Q = Q_0 + \epsilon Q_1 + \epsilon^2 Q_2 + \cdots,$$
$$(4.7)$$

and substitute the expansions in (4.5). Letting $\mathcal{S} = P_1 + Q_1$ and $\mathcal{D} = Q_1 - P_1$, the order $\epsilon$ gives

$$(-d^2/d\xi^2 + 1 - 6\operatorname{sech}^2\xi)\mathcal{S} = 0, \quad (4.8)$$

$$\left(-\frac{d^2}{d\xi^2} + 1 - \frac{2}{3}\operatorname{sech}^2\xi\right)\mathcal{D} = \frac{2}{9\sqrt{3}}\frac{\mu^{3/2}}{\omega_0}\operatorname{sech}^5\xi, \quad (4.9)$$

where we have defined $\xi = \mu^{1/2}X$.

The operator in the left-hand side of (4.8) has a zero eigenvalue, with the associated eigenfunction being odd. If we wish to construct a solution with definite parity (i.e., an even solution), we should take $\mathcal{S} = 0$. On the other hand, the operator in the left-hand side of (4.9) is positive definite and hence invertible. As a result, Eq. (4.9) has an exponentially decaying solution:

$$\mathcal{D} = \frac{1}{51\sqrt{3}}\frac{\mu^{3/2}}{\omega_0}(6\operatorname{sech}\xi + \operatorname{sech}^3\xi).$$

Taken together with $\mathcal{S} = 0$, this implies

$$Q_1 = -P_1 = \frac{1}{102\sqrt{3}}\frac{\mu^{3/2}}{\omega_0}(6\operatorname{sech}\xi + \operatorname{sech}^3\xi). \quad (4.10)$$

Returning to the original variables $u$ and $v$ we note that, as expected, the parameters $\epsilon$ and $\mu$ enter the solution only in combination, $\epsilon\mu$. Without loss of generality, we can set one of these to 1, e.g., $\mu = 1$.

Equations (4.3), with $P$ and $Q$ expanded as in (4.7), and $P_n$ and $Q_n$ as in (4.6) and (4.10), provide solutions to the amplitude equations (3.14):

$$p = \frac{e^{iT}}{\sqrt{3}}\operatorname{sech}X\left[1 - \frac{\epsilon}{102\omega_0}(6 + \operatorname{sech}^2 X) + O(\epsilon^2)\right],$$

$$q = \frac{e^{iT}}{\sqrt{3}}\operatorname{sech}X\left[1 + \frac{\epsilon}{102\omega_0}(6 + \operatorname{sech}^2 X) + O(\epsilon^2)\right].$$
$$(4.11)$$

Since both $p$ and $q$ are nonzero in (4.11), we will be referring to these solutions as *two-component* solitons.

Feeding Eqs. (4.11) into (3.5), (3.7), (3.9), and (3.12) gives

$$a = \epsilon^{1/2}[A_0 + \epsilon A_1 + O(\epsilon^2)], \quad b = \epsilon^{1/2}[B_0 + \epsilon B_1 + O(\epsilon^2)],$$
$$(4.12)$$

with

$$A_0 = \frac{e^{-i(\omega_0 - \epsilon)t}}{\sqrt{3}}\operatorname{sech}(\epsilon^{1/2}x)$$
$$\times\left[1 - \frac{\epsilon}{102\omega_0}[6 + \operatorname{sech}^2(\epsilon^{1/2}x)] + O(\epsilon^2)\right],$$

$$B_0 = \frac{e^{i(\omega_0 + \epsilon)t}}{\sqrt{3}}\operatorname{sech}(\epsilon^{1/2}x)$$
$$\times\left[1 + \frac{\epsilon}{102\omega_0}[6 + \operatorname{sech}^2(\epsilon^{1/2}x)] + O(\epsilon^2)\right],$$

$$A_1 = \frac{e^{i\epsilon t}}{6\sqrt{3}\omega_0}\operatorname{sech}^3(\epsilon^{1/2}x)$$
$$\times[e^{i(3\omega_0 t + 2\theta)} - 4i\gamma e^{-i(3\omega_0 t + \theta)}] + O(\epsilon),$$

$$B_1 = -\frac{e^{i\epsilon t}}{6\sqrt{3}\omega_0}\operatorname{sech}^3(\epsilon^{1/2}x)$$
$$\times[4i\gamma e^{i(3\omega_0 t + \theta)} + e^{-i(3\omega_0 t + 2\theta)}] + O(\epsilon). \quad (4.13)$$

Equations (4.12) and (4.13), taken together with the conversion formulas

$$u(x,t) = a + b, \quad v(x,t) = e^{i\theta}b - e^{-i\theta}a, \quad (4.14)$$

yield solutions of the original equation (2.1).

To test the accuracy of the asymptotic solution (4.12)–(4.14), we simulated equations (2.1) with the initial conditions in the form (4.12)–(4.14) with $t = 0$. [In these initial conditions, we neglected the $O(\epsilon^2)$ terms in $A_0, B_0$ and the $O(\epsilon)$ terms in $A_1, B_1$.] The resulting oscillatory configuration is plotted in Fig. 2. The fundamental harmonic in the frequency spectrum of $|u|^2$ and $|v|^2$ was indeed found to be very close to $2\omega_0$, the double frequency of the asymptotic solution.

As we mentioned in Sec. II, the system (2.1) may be thought of as a continuum limit of a chain of coupled $\mathcal{PT}$-symmetric dimers. The power in each dimer can perform a periodic oscillation [20,21], with an amplitude-dependent period. The breather is an oscillation involving the entire chain. Although the amplitude of oscillation varies along the chain, the coupling synchronizes individual dimers so that the breather has a single base frequency. Accordingly, the power integrals (2.2) associated with the two modes show a perfectly periodic behavior [Fig. 2(c)]. The total power $\mathcal{P}_u + \mathcal{P}_v$ is not a constant of motion but is periodic and therefore conserved on average.

## V. STABILITY

The amplitude equations (3.14) may be used to study the dynamics of the solitons and breathers of the original system (2.1) over times up to $t \sim \epsilon^{-2}$. In particular, Eqs. (3.14) may be used to study the stability of these objects.

Consider a stationary solution (4.3) of the system (3.14). This can be one of the two degenerate solitons (4.1) and (4.2)— or the nondegenerate soliton (4.7),(4.6),(4.10) corresponding to the breather of the original system (2.1). We consider the simplest situation where $\mu = \nu$; in this case we may set, without loss of generality, $\mu = \nu = 1$. Linearizing Eqs. (3.14) about the stationary solution and assuming perturbations of the form

$$\delta p(X,T) = e^{iT}[\text{f}(X,T) + i\text{g}(X,T)],$$
$$\delta q(X,T) = e^{iT}[\text{y}(X,T) + i\text{z}(X,T)],$$

where f, g, y, and z are real, gives

$$\begin{aligned}\mathcal{L}_1\text{f} + \mathcal{V}(X)\text{y} = -\text{g}_T, \qquad \mathcal{L}_0\text{g} = \text{f}_T, \\ \mathcal{M}_1\text{y} + \mathcal{V}(X)\text{f} = -\text{z}_T, \qquad \mathcal{M}_0\text{z} = \text{y}_T.\end{aligned} \quad (5.1)$$

Here we have introduced the operators

$$\mathcal{L}_0 = -\partial^2/\partial X^2 + 1 - 2P^2 - 4Q^2 + \frac{\epsilon}{\omega_0}(2P^2 - Q^2)Q^2,$$

$$\mathcal{L}_1 = -\partial^2/\partial X^2 + 1 - 6P^2 - 4Q^2 + \frac{\epsilon}{\omega_0}(6P^2 - Q^2)Q^2,$$

$$\mathcal{M}_0 = -\partial^2/\partial X^2 + 1 - 4P^2 - 2Q^2 + \frac{\epsilon}{\omega_0}(P^2 - 2Q^2)P^2,$$

$$\mathcal{M}_1 = -\partial^2/\partial X^2 + 1 - 4P^2 - 6Q^2 + \frac{\epsilon}{\omega_0}(P^2 - 6Q^2)P^2,$$

and a coefficient function

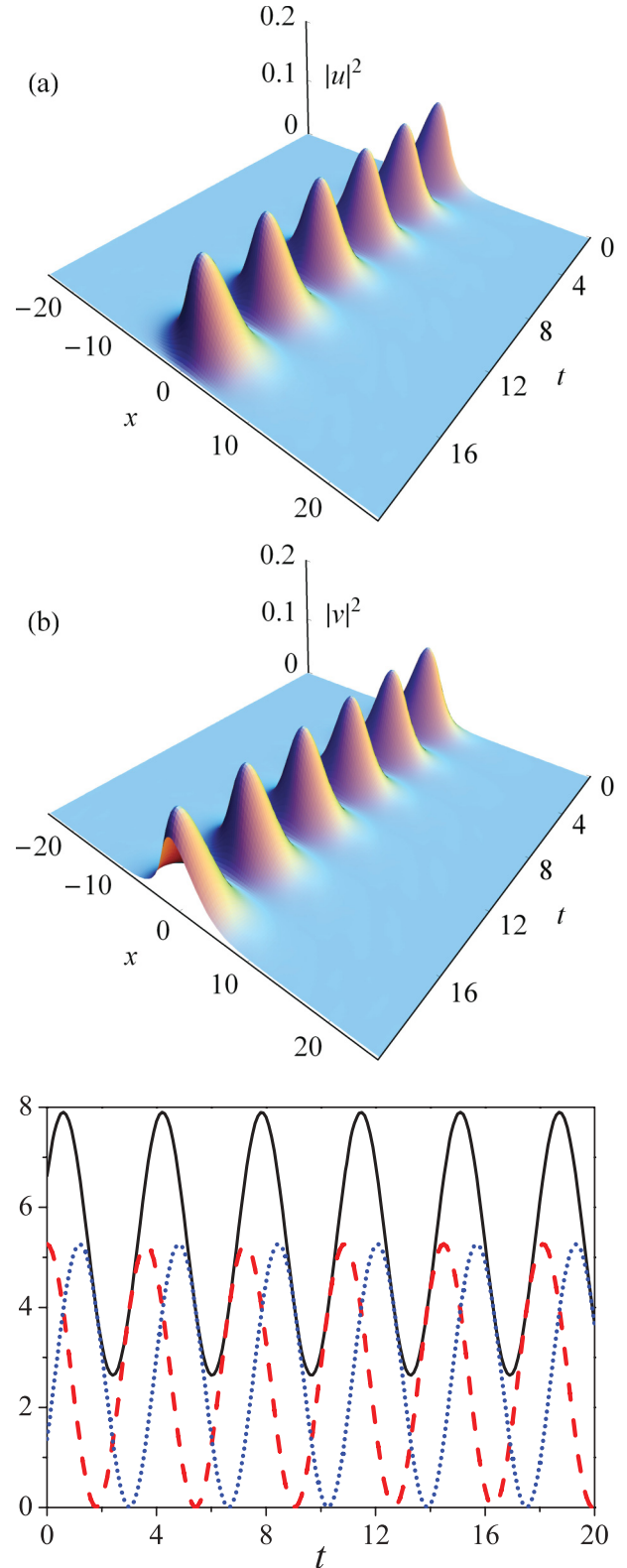$$\mathcal{V}(X) = -8PQ + \frac{4\epsilon}{\omega_0}(P^2 - Q^2)PQ.$$



FIG. 2. (Color online) Numerical evolution of the initial condition in the form of the expansion (4.12)–(4.14) with $t = 0$. (In this simulation, $\gamma = 0.5$ and $\epsilon = 0.1$.) Shown are $|u|^2$ (a), $|v|^2$ (b), and powers carried by the two components of the breather (c). In (c), $\mathcal{P}_u$ is depicted by the broken red and $\mathcal{P}_v$ by the dotted blue line. Also shown is the total power $\mathcal{P}_u + \mathcal{P}_v$ (solid line). The simulation continued until times much longer than $\epsilon^{-2} = 100$, without any visible change in the amplitude or period of the breather.

For separable solutions of the form

$$f(X,T) = \text{Re}[e^{\lambda T} f(X)], \quad g(X,T) = \text{Re}[e^{\lambda T} g(X)],$$
$$y(X,T) = \text{Re}[e^{\lambda T} y(X)], \quad z(X,T) = \text{Re}[e^{\lambda T} z(X)],$$

with complex $f$, $g$, $y$, $z$, and $\lambda$, Eq. (5.1) reduces to an eigenvalue problem:

$$\mathcal{A} \begin{pmatrix} \vec{y} \\ \vec{z} \end{pmatrix} = \lambda \begin{pmatrix} \vec{y} \\ \vec{z} \end{pmatrix}, \tag{5.2}$$

where

$$\mathcal{A} = \begin{pmatrix} 0 & \mathcal{H}_0 \\ -\mathcal{H}_1 & 0 \end{pmatrix} \tag{5.3}$$

is a $4 \times 4$ matrix with blocks given by

$$\mathcal{H}_0 = \begin{pmatrix} \mathcal{L}_0 & 0 \\ 0 & \mathcal{M}_0 \end{pmatrix}, \quad \mathcal{H}_1 = \begin{pmatrix} \mathcal{L}_1 & \mathcal{V}(X) \\ \mathcal{V}(X) & \mathcal{M}_1 \end{pmatrix},$$

and $\vec{y}$, $\vec{z}$ are two-component vectors:

$$\vec{y} = \begin{pmatrix} f \\ y \end{pmatrix}, \quad \vec{z} = \begin{pmatrix} g \\ z \end{pmatrix}. \tag{5.4}$$

### A. Stability of the high- and low-frequency solitons

Consider, first, the degenerate soliton (4.1) and let the velocity $V = 0$. [This degenerate soliton with $Q = 0$ describes the amplitude of the low-frequency soliton of the original $\mathcal{PT}$-symmetric equations (2.1).] In this case, the operators $\mathcal{L}_0$ and $\mathcal{L}_1$ reduce to $L_0$ and $L_1$, respectively, where

$$L_0 = -d^2/dX^2 + 1 - 2\,\text{sech}^2 X, \tag{5.5}$$

$$L_1 = -d^2/dX^2 + 1 - 6\,\text{sech}^2 X, \tag{5.6}$$

while $\mathcal{M}_0$ and $\mathcal{M}_1$ acquire a common form which we denote $L_{1/2}$:

$$L_{1/2} = -\frac{d^2}{dX^2} + 1 - 4\,\text{sech}^2 X + \frac{\epsilon}{\omega_0}\,\text{sech}^4 X. \tag{5.7}$$

Since $Q = 0$ implies $\mathcal{V}(X) = 0$, the eigenvalue problem (5.2) acquires a block-diagonal form:

$$L_0 g = \lambda f, \quad L_1 f = -\lambda g, \tag{5.8}$$

$$L_{1/2} y = -\lambda z, \quad L_{1/2} z = \lambda y. \tag{5.9}$$

Equation (5.8) is the linearized eigenvalue problem for the scalar cubic nonlinear Schrödinger equation, a well-researched integrable system. It has no discrete eigenvalues except the fourfold zero eigenvalue. Its continuous spectrum occupies the imaginary axis.

On the other hand, Eq. (5.9) gives

$$L_{1/2}^2 y = -\lambda^2 y.$$

This implies that $\lambda = i\omega$, where $\omega$ is an eigenvalue of the Hermitian operator $L_{1/2}$. Since all such eigenvalues are real, all $\lambda$'s are purely imaginary and hence the degenerate soliton is stable.

When $\epsilon = 0$, the operator $L_{1/2}$ has two discrete eigenvalues $\omega_a$ and $\omega_b$ given by

$$\omega_a = \alpha - 3 \approx -1.438, \quad \omega_b = 3\alpha - 4 \approx 0.685, \tag{5.10}$$

with $\alpha = (\sqrt{17} - 1)/2$. The corresponding eigenfunctions are $\psi_a = \text{sech}^\alpha X$ and $\psi_b = \text{sech}^{\alpha-1} X \tanh X$, respectively. The eigenvalues $\omega_a$ and $\omega_b$ persist when $\epsilon$ deviates from zero (but remains finitely small). It is only when $\epsilon$ grows above a certain finite value that $\omega_b$ and then $\omega_a$ become immersed in the continuous spectrum. Accordingly, for $\epsilon$ below a finite threshold, the degenerate soliton (4.1) has two modes of internal oscillation. (For $\epsilon = 0$, this fact has been established in [53].)

The degenerate soliton (4.2) corresponds to the high-frequency soliton of the original equations (2.1). The linearization about this degenerate soliton leads to the same eigenvalue problem (5.9), with the same operator (5.7), where one just needs to replace $\epsilon \to -\epsilon$. This observation establishes the stability of the soliton (4.2). As long as $\epsilon$ remains below a finite threshold, the operator $L_{1/2}$ with $\epsilon \to -\epsilon$ has two discrete eigenvalues; hence the degenerate soliton (4.2) has two internal modes.

The fact that the degenerate solitons of the amplitude equations (3.14) are stable implies that both the low- and high-frequency solitons of the $\mathcal{PT}$-symmetric system (2.1) are stable for sufficiently small $\epsilon$. This conclusion is in agreement with the analysis of the low- and high-frequency solitons performed directly on Eqs. (2.1). Namely, the high-frequency soliton was shown to be stable when its amplitude $a$ lies below a finite threshold $a_c$, $a_c = (\frac{2}{3})^{1/2}(1 - \gamma^2)^{1/4}$ [35,37]. On the other hand, the low-frequency soliton has an unstable eigenvalue irrespective of the amplitude but its real part is exponentially small when the amplitude is small [37]. This instability constitutes an effect that lies beyond all orders in $\epsilon^n$; it cannot be captured by the amplitude equations (3.14). The unstable perturbations take an exponentially long time to grow in this case; hence the small-amplitude low-frequency soliton will not reveal any instability when studied over time intervals $t \sim \epsilon^{-n}$.

The frequencies of the internal modes of the low- and high-frequency soliton solutions of Eqs. (2.1) were also computed in [37]. These coincide with the frequencies (5.10) computed using the amplitude equations (3.14).

### B. Stability and spectrum of the breather: $t \sim \epsilon^{-1}$

Turning to the two-component soliton (4.11), it is convenient to consider the soliton of the "curtailed" system (3.15) first. The stability of the soliton of the system (3.15) will imply the stability of the breather of the original $\mathcal{PT}$-symmetric system (2.1) over time intervals $t \sim \epsilon^{-1}$ (where $\epsilon^{1/2}$ is the amplitude of the breather).

The two-component soliton of the system (3.15) is given by Eqs. (4.11) with $\epsilon = 0$:

$$p = \frac{1}{\sqrt{3}} e^{iT}\,\text{sech} X, \quad q = \frac{1}{\sqrt{3}} e^{iT}\,\text{sech} X. \tag{5.11}$$

Depending on the context, this symmetric solution has been referred to as the *linearly polarized* [48] or *equally mixed* [51] soliton. Note that setting $\epsilon = 0$ in Eqs. (4.11) does not mean that we are considering breathers of zero amplitude. The nonzero parameter $\epsilon$ remains present in the corresponding breather solution (4.12),(4.13),(4.14); in particular the amplitude of the breather remains equal to $\epsilon^{1/2} \neq 0$.

The stability of the soliton (5.11) was proved by the construction of a Lyapunov functional [46]. With an eye to addressing the situation of general $\epsilon$, we reconsider the stability of this solution here—using the eigenvalue analysis.

When $\epsilon = 0$, the eigenvalue problem (5.2) can be cast in the block-diagonal form

$$\begin{pmatrix} 0 & -L_1 \\ L_0 & 0 \end{pmatrix} \begin{pmatrix} \zeta_1 \\ \zeta_2 \end{pmatrix} = \lambda \begin{pmatrix} \zeta_1 \\ \zeta_2 \end{pmatrix}, \qquad (5.12)$$

$$\begin{pmatrix} 0 & -L_+ \\ L_0 & 0 \end{pmatrix} \begin{pmatrix} \rho_1 \\ \rho_2 \end{pmatrix} = \lambda \begin{pmatrix} \rho_1 \\ \rho_2 \end{pmatrix}, \qquad (5.13)$$

where the operators $L_0$ and $L_1$ are as in (5.5) and (5.6), and

$$L_+ = -\frac{d^2}{dX^2} + 1 - \frac{2}{3}\operatorname{sech}^2 X. \qquad (5.14)$$

The components of the column vectors in (5.12) and (5.13) are the sums and differences of the components of the vectors in (5.4): $\zeta_1 = z + g$, $\zeta_2 = y + f$, $\rho_1 = z - g$, $\rho_2 = y - f$.

Equation (5.12) arose in the previous section [see Eq. (5.8)]. It is the linearized eigenvalue problem for the scalar cubic nonlinear Schrödinger equation. As discussed there, the matrix-differential operator (5.12) does not have any discrete eigenvalues except the four zeros. Therefore Eq. (5.12) can be safely disregarded and we can focus on Eq. (5.13).

In order to transform Eq. (5.13) to a form more amenable to analysis, we note that the only discrete eigenvalue of the operator (5.14) is $\beta + 1/3$, where $\beta = \sqrt{11/12} - 1/2 > 0$. (It is associated with the nodeless eigenfunction $\psi = \operatorname{sech}^\beta X$.) Hence the operator $L_+$ is positive definite and admits an inverse. This observation allows us to write the vector equation (5.13) as a generalized eigenvalue problem for a pair of scalar operators,

$$L_0 \rho_1 = -\lambda^2 L_+^{-1} \rho_1. \qquad (5.15)$$

In (5.15), $L_0$ is a symmetric operator, and $L_+^{-1}$ is symmetric and positive definite. All eigenvalues $(-\lambda^2)$ of the problem (5.15) are real and the corresponding eigenfunctions can also be chosen real. The lowest eigenvalue $-\lambda_0^2$ can be found as the minimum of the Rayleigh quotient:

$$-\lambda_0^2 = \min \frac{(\rho_1, L_0 \rho_1)}{(\rho_1, L_+^{-1} \rho_1)}. \qquad (5.16)$$

Here $(\,,)$ stands for the scalar product in the space of square integrable real functions: $(\phi, \psi) = \int_{-\infty}^{\infty} \phi(X) \psi(X) dX$.

The lowest eigenvalue of the Schrödinger operator $L_0$ is zero; it is associated with the nodeless eigenfunction $z^{(0)}(X) = \operatorname{sech} X$. Therefore the Rayleigh quotient in (5.16) cannot take negative values and its minimum is exactly zero: $-\lambda_0^2 = 0$. This means that the matrix-differential operator in the left-hand side of (5.13) does not have any nonzero real eigenvalues $\lambda$ and so the soliton (5.11) of the vector nonlinear Schrödinger equation (3.15) is stable.

This is the main conclusion of this subsection. It implies that the small-amplitude breather of the $\mathcal{PT}$-symmetric system (2.1) is stable over time intervals $t \sim \epsilon^{-1}$.

In fact it is not difficult to show that the operator (5.13) does not have any discrete eigenvalues at all—neither real nor imaginary. (See Appendix B.) The implication is that when $\epsilon = 0$, the two-component soliton of the vector nonlinear

Schrödinger equation does not have internal modes. (This fact has been previously established by numerical means [53].) With regard to the breather of the $\mathcal{PT}$-symmetric system (2.1), this implies that the small-amplitude breather cannot have any modulating frequencies of order $\epsilon$ in its spectrum. This is the second conclusion of this subsection.

### C. Stability of the breather: $t \sim \epsilon^{-2}$

To extend the breather stability result to times of order $\epsilon^{-2}$, we need to consider the system (3.14) with $\epsilon \neq 0$. We should demonstrate that its solution (4.11) does not have unstable eigenvalues with Re$\lambda$ of order $\epsilon^\sigma$, $0 < \sigma \leqslant 1$, in its spectrum.

We begin the stability analysis of this solution with the identification of symmetries of the system (3.14). These will provide information on zero eigenvalues of the operator (5.3).

Besides the translation and Galilean invariance, the system (3.14) is symmetric with respect to U(1) × U(1) transformations of the form $p \to p e^{i\phi}$, $q \to q e^{i\chi}$, where $\phi, \chi = $ const. In addition, $\mu$ and $\nu$ can be chosen arbitrarily in the stationary system (4.4). Thus each solution of the form (4.3) is a member of a six-parameter continuous family and therefore the eigenvalue problem (5.2) has six zero eigenvalues.

The corresponding eigenvectors and generalized eigenvectors of the matrix $\mathcal{A}$ can be found explicitly. First, we observe that

$$\mathcal{H}_0 \begin{pmatrix} P \\ 0 \end{pmatrix} = \mathcal{H}_0 \begin{pmatrix} 0 \\ Q \end{pmatrix} = 0, \qquad (5.17)$$

and $\mathcal{H}_1 (P_X, Q_X)^T = 0$; hence $(P, 0, 0, 0)^T$, $(0, Q, 0, 0)^T$, and $(0, 0, P_X, Q_X)^T$ are the U(1) and translational eigenvectors, respectively. One can also check that $\mathcal{H}_1 (P_\mu, Q_\mu)^T = -(P, 0)^T$, $\mathcal{H}_1 (P_\nu, Q_\nu)^T = -(0, Q)^T$, and $\mathcal{H}_0 \vec{w} = (P_X, Q_X)^T$, where $\vec{w} = -\frac{1}{2} X (P, Q)^T$. These define the generalized eigenvectors: $(0, 0, P_\mu, Q_\mu)^T$, $(0, 0, P_\nu, Q_\nu)^T$, and $-\frac{1}{2} X (P, Q, 0, 0)^T$.

All nonzero eigenvalues $\lambda$ of the matrix $\mathcal{A}$ can be found from the solution of the eigenvalue problem for a $2 \times 2$ matrix:

$$\mathcal{H}_0 \mathcal{H}_1 \begin{pmatrix} f \\ y \end{pmatrix} = -\lambda^2 \begin{pmatrix} f \\ y \end{pmatrix}. \qquad (5.18)$$

Using (5.17) one can readily check that the eigenvectors of $\mathcal{H}_0 \mathcal{H}_1$ corresponding to $-\lambda^2 \neq 0$ satisfy

$$\int f(X) P(X) dX = \int y(X) Q(X) dX = 0.$$

These orthogonality constraints define a subspace of the space of square integrable vector functions. On this subspace, the operator $\mathcal{H}_0$ admits an inverse and (5.18) can be written as

$$\mathcal{H}_1 \begin{pmatrix} f \\ y \end{pmatrix} = -\lambda^2 \mathcal{H}_0^{-1} \begin{pmatrix} f \\ y \end{pmatrix}. \qquad (5.19)$$

The components $P(X)$ and $Q(X)$ of the solution (4.7) remain positive for all $X$ as long as $\epsilon$ remains below a finite threshold. This means that zero remains the lowest eigenvalue of the operators $\mathcal{L}_0$ and $\mathcal{M}_0$—the operators whose null eigenvectors are given by $P$ and $Q$. Therefore, the operator $\mathcal{H}_0^{-1}$ remains positive definite (and symmetric) while the operator $\mathcal{H}_1$ is symmetric. Equation (5.19) implies then that all eigenvalues $(-\lambda^2)$ are real, so that all $\lambda$ are either real or purely imaginary.

As $\epsilon$ grows from zero, the six eigenvalues of the matrix $\mathcal{A}$ remain at the origin. New discrete eigenvalues can arise only by bifurcating from the continuous spectrum which fills the imaginary axis of $\lambda$ outside the gap $(-i, +i)$. Once an eigenvalue has detached from the continuum, it can move along the imaginary axis toward the origin. However, the eigenvalue can reach the origin only if $\epsilon$ exceeds a finite threshold. Therefore, the two-component soliton will remain stable as long as $\epsilon$ remains (finitely) small.

Concerning the breather solution of the system (2.1), the implication of this result is that the $\mathcal{PT}$-symmetric breather is stable on the time scale $t \lesssim \epsilon^{-2}$. (That is, the breather's lifetime is no shorter than $\epsilon^{-2}$.)

## VI. BREATHER PRODUCTION IN SOLITON COLLISIONS

Breathers are known not to be exceptional or isolated occurrences in the $\mathcal{PT}$-symmetric planar coupler. In particular, they form as a result of the soliton instability [37,56]. In this section we argue that breathers are even more common than solitons themselves: a collision of a high- and a low-frequency soliton produces two or more breathers, and a collision of two breathers also results in one or more of these oscillatory objects.

We use Eqs. (2.1) to simulate the evolution of the initial condition in the form of two solitons of equal amplitudes, moving toward each other with equal velocities:

$$u(x,0) = a + b, \quad v(x,0) = e^{i\theta}b - e^{-i\theta}a,$$
$$a = e^{i(v/2)(x+x_0)}\sqrt{\mu}\,\mathrm{sech}[\sqrt{\mu}(x+x_0)], \quad (6.1)$$
$$b = e^{-i(v/2)(x-x_0)}\sqrt{\mu}\,\mathrm{sech}[\sqrt{\mu}(x-x_0)].$$

Taking $x_0 > 0$, the low-frequency soliton is initially on the left and the high-frequency one is on the right; the initial velocities are $v$ and $-v$, respectively. [Note that in (6.1), the same symbol $v$ denotes the velocity of the soliton and the second component of the vector field, $v(x,t)$; this slight abuse of notation should cause no confusion.] The initial distance between the solitons is assumed to be much larger than their widths: $2\sqrt{\mu}x_0 \gg 1$.

The high-frequency soliton is stable if $\mu \leqslant \frac{2}{3}\sqrt{1-\gamma^2}$ [35,37]. The low-frequency soliton is unstable for all $\mu$ but when the amplitude is small, its instability growth rate is exponentially small in $\mu$ [37]. Therefore when the solitons' amplitudes are sufficiently small, the low-frequency soliton will not manifest instability in the run-up to the collision. The two small-amplitude solitons can be considered as two stable entities.

The collision of the low-frequency and the high-frequency solitons in the $\mathcal{PT}$-symmetric system (2.1) corresponds to the collision of degenerate solitons (4.1), (4.2) governed by the amplitude equations (3.14). In the particular case $\epsilon = 0$, such collisions were studied by Tan and Yang [55] (see also [51]). Depending on the solitons' initial velocities, the colliding degenerate solitons were recorded to pass through each other or bounce back. The solitons emerging from the collision would no longer be degenerate; instead, they would have both $p$ and $q$ components nonzero [51,55]. Translated into the language of the $\mathcal{PT}$ system (2.1), this means that the collision of the small-amplitude $\mathcal{PT}$ solitons should typically result in the emergence of two breathers.
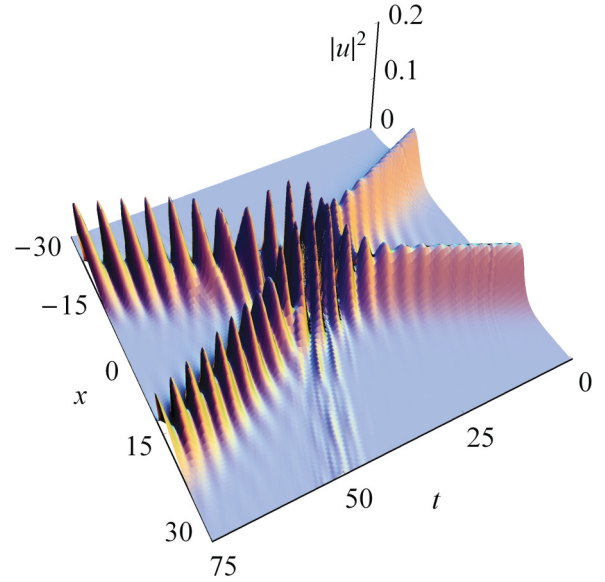


FIG. 3. (Color online) The collision of the low- (initially on the left) and the high-frequency (initially on the right) solitons. As the solitons approach each other, they develop beat-frequency oscillations of growing amplitude. The localized objects emerging from the collision remain oscillatory despite the growing separation distance—these are a pair of breathers. The breathers are weakly radiating; also note the emission of a rapid small-amplitude breather at the moment of collision. In this simulation, $\gamma = 0.5$, $\sqrt{\mu} = 0.3$, $v = 0.4$, and $x_0 = 16$.

This is indeed the scenario that we have observed in our numerical simulations of Eqs. (2.1). We have detected the formation of two breathers in collisions of small- and moderate-amplitude solitons. A typical evolution is depicted in Fig. 3.

An interesting feature of the degenerate-soliton collisions recorded by Tan and Yang [55] was that the reduction of the collision velocity did not result in the decrease of the velocities of the solitons after collision. In agreement with this amplitude-equation effect, our simulations of the collision of $\mathcal{PT}$ solitons with initial velocities $v \to 0$ have produced breathers diverging at finite speeds [see, e.g., Figs. 4(a) and 4(b)].

Another inelastic effect detected in the curtailed amplitude equation (3.15) pertained to the initial velocities in the range $0.1 < V < 0.3$. For these $V$, the collision of two degenerate solitons was seen to result in the production of a stationary small-amplitude soliton, in addition to the two transmitted or reflected ones [55]. A similar phenomenon accompanies the collision of the low- and high-frequency small-amplitude solitons in our $\mathcal{PT}$-symmetric system (2.1). Namely, the initial condition (6.1) with $v$ in the range $0.1\mu^{1/2} < v < 0.3\mu^{1/2}$ and small $\mu$ gives rise to three breathers. Two of these move apart while the third, small-amplitude, breather is left behind near the origin. We have observed this effect even for not-very-small soliton amplitudes [Fig. 4(a)].

As the amplitudes of the colliding solitons are increased, the curtailed equation (3.15) ceases to be applicable. The collision of larger-amplitude solitons is now accompanied by intense radiation, while the oscillations of the emerging
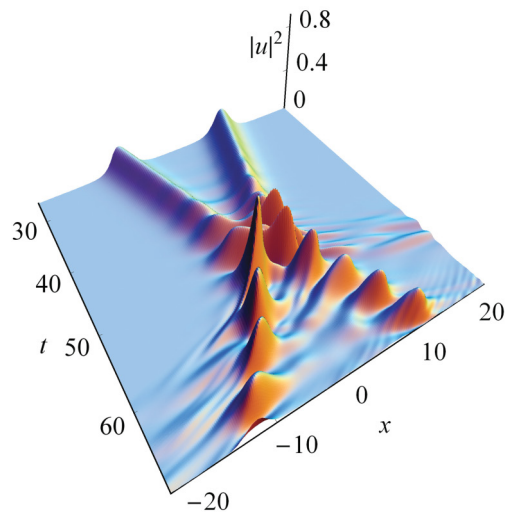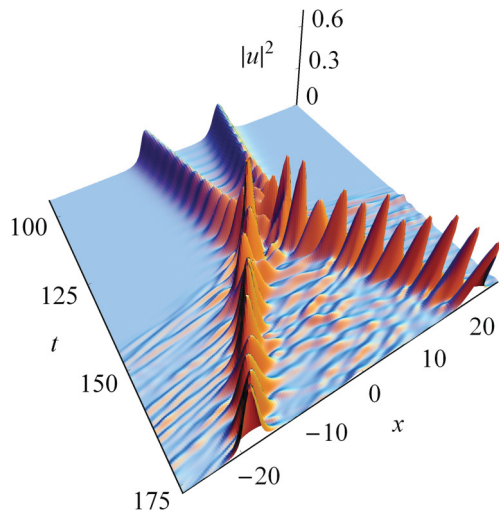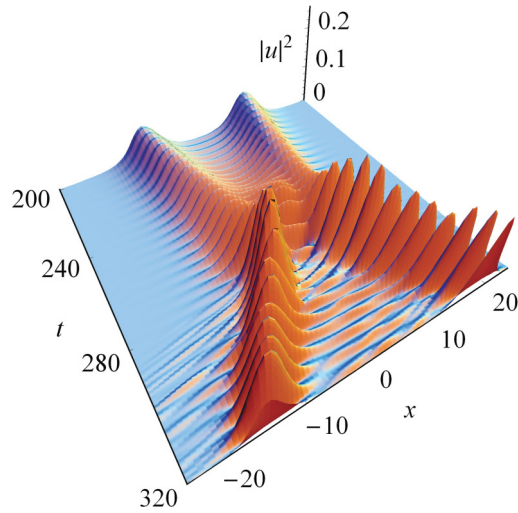
breathers acquire a low-frequency modulation [Fig. 4(b)]. As the amplitudes exceed a certain threshold, the collision results in a blowup of one of the fragments.

One more range of parameter values where the equation (3.15) does not furnish any accurate description of the dynamics pertains to large $v$. As $v$ is increased, we observe the growth of the transient amplitude of one of the emerging breathers—a kind of a rogue wave appearing just after the collision [Fig. 4(c)]. Eventually, this rogue wave seeds the blowup of the breather.

It is worth emphasizing here that the creation of breathers is characteristic only for the collision of two solitons of different types (that is, collision of the low- with the high-frequency soliton). The scattering of two *like* solitons, e.g., two high-frequency solitons, is purely elastic—for the simple reason that the initial condition and the resulting solution belong to the

FIG. 4. (Color online) The collision of solitons with moderate and large amplitudes, small and large initial velocities. In (a), $\gamma = 0.6$, $\sqrt{\mu} = 0.3$, and the initial velocity $v = 0.075$ lies in the interval $(0.1\mu^{1/2}, 0.3\mu^{1/2})$. Note a small-amplitude nonpropagating breather left behind while two large-amplitude fragments shoot out of the collision. (b) shows the collision of solitons with larger amplitudes. Here $\gamma = 0.5$, $\sqrt{\mu} = 0.5$, and $v = 0.125$. (c) corresponds to large initial velocities: $\gamma = 0.5$, $\sqrt{\mu} = 0.25$, and $v = 0.6$.
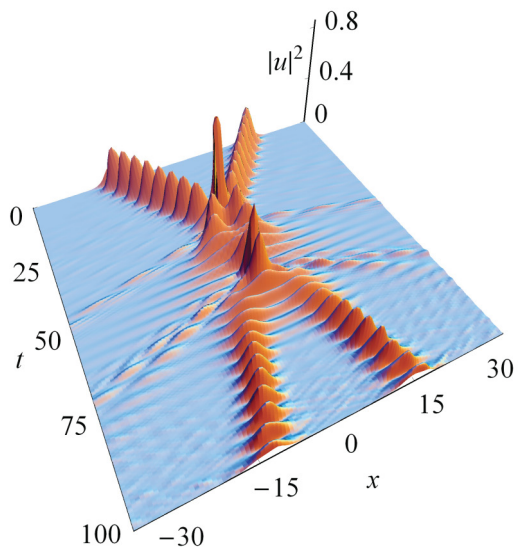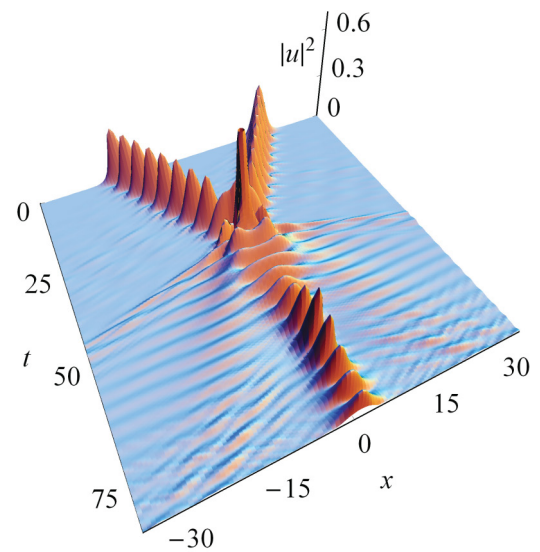
FIG. 5. (Color online) The collision of two breathers. Both breathers are taken in the form (4.12),(4.13),(4.14), with the amplitudes $\sqrt{\epsilon} = 0.3$, and Galileo boosted with the velocities $v = \pm 0.5$. (a) and (b) are different in the initial phase of the breathers. In both plots, $\gamma = 0.3$.

same invariant manifold $a = 0$. The constraint $a = 0$ defines a reduction to a completely integrable equation [Eq. (3.4)]; hence the elasticity of collisions.

The ubiquity of the breathers stems from the fact that they are not confined to the $a = 0$ or $b = 0$ manifold. They represent trajectories evolving out of generic initial conditions which do not belong to either of the two reductions.

Finally, we touch upon the collision of two breathers. The outcome of this collision can be predicted on the basis of the amplitude equation (3.14). Indeed, the scattering of two generic solitons in a Hamiltonian system typically produces two solitons of lower energy, or their bound state. Consistently with these expectations, the numerical simulations of Eqs. (2.1) demonstrate the production of one or two breathers (Fig. 5).

## VII. CONCLUDING REMARKS

Stationary solitons in the $\mathcal{PT}$-symmetric planar coupler are known to be sustained due to the exact offsetting of the power gained in the active waveguide by the power lost in its passive counterpart [34,35,37]. In this paper, we have described another realization of the gain-loss balance, which is provided by the breathers. In the breather case, the total power is conserved not at every moment in time, but only over a period of oscillation.

The results of our study can be summarized as follows.

(1) We have derived a system of amplitude equations [Eqs. (3.14)] governing the envelope of the breather. For times $t \lesssim \epsilon^{-2}$, where $\epsilon^{1/2}$ gives the scale of the amplitude of the small-amplitude breather, the system (3.14) is equivalent to the original system (2.1).

(2) Despite the fact that the original $\mathcal{PT}$-symmetric system includes gain and loss, the amplitude system was shown to be conservative.

(3) The breather solution was constructed as the asymptotic expansion (4.12), (4.13), and (4.14).

(4) We have proved that all small-amplitude breathers are stable on the time scale $t \lesssim \epsilon^{-2}$. The small-amplitude breather was shown to be a "simple" oscillation—it cannot have any modulating frequencies in its spectrum.

(5) Breathers were shown to be common occurrences in $\mathcal{PT}$-symmetric chains of dimers. In particular, breathers are created in collisions of low- and high-frequency solitons.

In conclusion, we need to make three remarks. The first one concerns the $\mathcal{PT}$ breathers versus conservative breathers and limit cycles. The $\mathcal{PT}$-symmetric breathers are different from their conservative counterparts in that their associated physical observables (e.g., energy and momentum) are not stationary but oscillate in time. From this point of view, the $\mathcal{PT}$ breathers are similar to the time-periodic solitons in dissipative systems [57–59]. However, there is an important distinction between the latter two categories too. Namely, the dissipative solitons are limit cycles (in an infinite-dimensional phase space); their amplitudes and periods are determined uniquely by the parameters of the system. On the contrary, the $\mathcal{PT}$ breathers arise as members of two-parameter families, similar to periodic trajectories in Hamiltonian systems.

The second remark is on the radiation from the breather. Using the singular perturbation expansion, the breather can be constructed to any order in $\epsilon$. All higher-order corrections
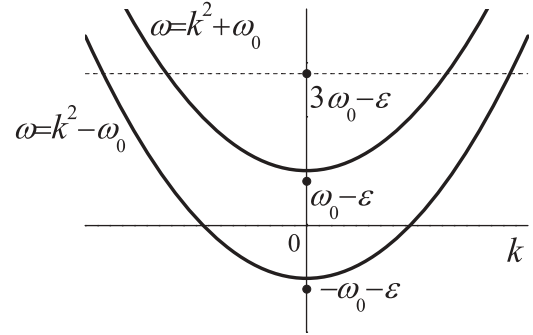


FIG. 6. The dispersion curves of the $\mathcal{PT}$-symmetric system (2.1). The black dots indicate the two frequencies of the breather. The dashed line marks the frequency of radiation.

$A_n, B_n$ are expressible as powers of $A_0, B_0$ and decay to zero as $|x| \to \infty$. There is no radiation to any order $\epsilon^n$, $n = 0, 1, 2, 3, \ldots$.

However our simulations do reveal radiation waves from the breathers, with the amplitude of the waves growing as the amplitude of the breather is increased. The reason why the asymptotic expansion does not capture these waves is that the amplitude of the radiation is exponentially small in $\epsilon$. (The exponential smallness does not imply that the radiation is invisible for *finitely* small $\epsilon$ though.)

The frequency of the radiation can be determined on the basis of standard considerations. Indeed, the spectrum of linear excitations of the system (3.2) consists of two branches $\omega = k^2 + \omega_0$ and $\omega = k^2 - \omega_0$ (Fig. 6), while the breather of amplitude $\epsilon^{1/2}$ has two basic frequencies $\omega_0 - \epsilon$ and $-\omega_0 - \epsilon$ [see Eq. (4.13)]. The term $a^2 b^*$ in (3.2) oscillates at a combination frequency $3\omega_0 - \epsilon$ which falls in the linear spectrum. Hence the dominant frequency of the resonant radiation will be $3\omega_0 - \epsilon$, as indicated by the dashed line in Fig. 6. (Note that the frequency $\omega_0 - \epsilon$ does not resonate with the bottom branch since the $a$ and $b$ modes are not coupled to linear order.)

Finally, we note that the breathers realize periodic light switching between the waveguides with gain and loss. Unlike oscillations in structureless linear [12,13] and nonlinear [20,21] $\mathcal{PT}$ couplers, the breathers describe switching between spatially extended waveguides. Here, the nonlinearity suppresses the beam diffraction while the spatial coupling synchronizes the power oscillations across the beam.

## APPENDIX A: MORE GENERAL BREATHER SOLUTIONS

In this appendix, we briefly comment on other solutions of the system (4.4)—more general than the nearly symmetric configuration (4.7), (4.6), (4.10). By rescaling $P$, $Q$, and $X$ and redefining $\epsilon$, we can always arrange that $\mu = 1$ in Eqs. (4.4):

$$P'' - P + 2(|P|^2 + 2|Q|^2)P + \frac{\epsilon}{\omega_0}(|Q|^4 - 2|PQ|^2)P = 0,$$

$$Q'' - \nu Q + 2(|Q|^2 + 2|P|^2)Q + \frac{\epsilon}{\omega_0}(2|PQ|^2 - |P|^4)Q = 0.$$
(A1)

Note that we are not setting $\nu$ equal to 1, along with $\mu$.

For $\epsilon = 0$, the system (A1) has even and odd solutions with $n$ humps ($n = 1, 2, \ldots$), with both $P$ and $Q$ being nonzero [48,52]. Each of these can be used as a starting point in the regular perturbation expansion in powers of $\epsilon$.

In particular, the solution of the system (A1) with $\epsilon = 0$, with an even single-humped $P(X)$ and an even single-humped $Q(X)$, exists for $\alpha^{-2} < \nu < \alpha^2$, where $\alpha^2 = \frac{1}{4}(\sqrt{17} - 1)^2 \approx 2.438$ and $\alpha^{-2} \approx 0.410$ [49,52]. Therefore the system (A1) with sufficiently small *nonzero* $\epsilon$ will also have a localized solution for any $\nu$ between $\alpha^{-2}$ and $\alpha^2$.

The solution with a two-humped even $P(X)$ and a two-humped odd $Q(X)$ exists for $\beta^2 < \nu < 1$, where $\beta^2 = \frac{1}{4}(\sqrt{17} - 3)^2 \approx 0.315$ [49,52].

All these solitonlike solutions of the system (4.4) give rise to breather solutions of the $\mathcal{PT}$-symmetric system (2.1). Thus for each $n \geqslant 1$, the system (2.1) has a two-parameter family of nonpropagating breather solutions with $n$ humps. Representatives of the family are different in the amplitude and width of the humps, as well as the contrast of the $|u|^2$ and $|v|^2$ oscillations.

## APPENDIX B: NO INTERNAL MODES FOR THE SMALL-AMPLITUDE BREATHER

The aim of this appendix is to show that the operator (5.13) does not have any discrete eigenvalues. To this end, we note that if $\lambda \neq 0$, the bottom component of (5.13) gives

$$\int \rho_2(X) z^{(0)}(X) dX = 0,$$
(B1)

where $z^{(0)} = \mathrm{sech} X$ is the null eigenvector of the operator $L_0$. The constraint (B1) defines a subspace of the space of square integrable functions; we will denote this subspace $\mathfrak{S}$.

On the subspace $\mathfrak{S}$, the operator $L_0$ is positive definite; hence we can write (5.13) as another scalar eigenvalue problem, alternative to (5.15):

$$L_+ \rho_2 = -\lambda^2 L_0^{-1} \rho_2, \quad \rho_2 \in \mathfrak{S}.$$
(B2)

Assume that the nonsymmetric matrix-differential operator in (5.13) has nonzero eigenvalues $\lambda_1, \lambda_2, \ldots$. The corresponding eigenvalues $-\lambda_1^2 < -\lambda_2^2 < \cdots$ of (B2) are real, and the associated eigenfunctions $\rho_2(X)$ can also be chosen real. The lowest eigenvalue can be found as the minimum of the Rayleigh quotient:

$$-\lambda_1^2 = \min_{\mathfrak{S}} \frac{(\rho_2, L_+ \rho_2)}{(\rho_2, L_0^{-1} \rho_2)}.$$
(B3)

Since both $L_+$ and $L_0$ are positive definite, Eq. (B3) implies that the eigenvalue $-\lambda_1^2$ of the generalized eigenvalue problem (B2) is positive. Hence $\lambda_1$ lies in the gap of the continuous spectrum of the operator (5.13): $\lambda_1 = i\omega_1, -1 < \omega_1 < 1$.

On the other hand, any function from $\mathfrak{S}$ can be expanded over the continuous-spectrum eigenfunctions of the operator $L_0$:

$$\rho_2(X) = \int \mathcal{R}(k) z_k(X) dk,$$
(B4)

where $L_0 z_k = (1 + 2k^2) z_k, -\infty < k < \infty$. Writing $L_+$ as $L_0 + \frac{4}{3} \mathrm{sech}^2 X$ and substituting (B4) in (B3), the Rayleigh quotient becomes

$$\frac{\int \mathcal{R}^2(k)(1 + 2k^2) dk + \frac{4}{3} \int \rho_2^2 \, \mathrm{sech}^2 X \, dX}{\int \mathcal{R}^2(k)(1 + 2k^2)^{-1} dk}.$$
(B5)

The first term in the numerator of (B5) is greater than the denominator; hence the quotient is greater than 1. This contradicts the fact that the eigenvalue $\lambda_1$ is in the gap of the continuous spectrum of the operator (5.13). The contradiction proves that the operator (5.13) cannot have discrete eigenvalues.

[1] C. M. Bender and S. Boettcher, Phys. Rev. Lett. **80**, 5243 (1998).

[2] C. M. Bender, Rep. Prog. Phys. **70**, 947 (2007).

[3] A. Ruschhaupt, F. Delgado, and J. G. Muga, J. Phys. A **38**, L171 (2005).

[4] R. El-Ganainy, K. G. Makris, D. N. Christodoulides, and Z. H. Musslimani, Opt. Lett. **32**, 2632 (2007).

[5] S. Klaiman, U. Günther, and N. Moiseyev, Phys. Rev. Lett. **101**, 080402 (2008).

[6] K. G. Makris, R. El-Ganainy, D. N. Christodoulides, and Z. H. Musslimani, Phys. Rev. Lett. **100**, 103904 (2008).

[7] M. C. Zheng, D. N. Christodoulides, R. Fleischmann, and T. Kottos, Phys. Rev. A **82**, 010103 (2010).

[8] M. V. Berry, J. Phys. A **41**, 244007 (2008).

[9] S. Longhi, Phys. Rev. A **81**, 022102 (2010).

[10] S. Longhi, Phys. Rev. Lett. **103**, 123601 (2009).

[11] O. Bendix, R. Fleischmann, T. Kottos, and B. Shapiro, Phys. Rev. Lett. **103**, 030402 (2009).

[12] C. E. Ruter, K. G. Makris, R. El-Ganainy, D. N. Christodoulides, M. Segev, and D. Kip, Nat. Phys. **6**, 192 (2010).

[13] A. Guo, G. J. Salamo, D. Duchesne, R. Morandotti, M. Volatier-Ravat, V. Aimez, G. A. Siviloglou, and D. N. Christodoulides, Phys. Rev. Lett. **103**, 093902 (2009).

[14] H. Ramezani, T. Kottos, V. Kovanis, and D. N. Christodoulides, Phys. Rev. A **85**, 013818 (2012).

[15] A. E. Miroshnichenko, B. A. Malomed, and Yu. S. Kivshar, Phys. Rev. A **84**, 012123 (2011).

[16] C. T. West, T. Kottos, and T. Prosen, Phys. Rev. Lett. **104**, 054102 (2010).

[17] A. A. Sukhorukov, S. V. Dmitriev, S. V. Suchkov, and Yu. S. Kivshar, Opt. Lett. **37**, 2148 (2012).

[18] A. Regensburger, C. Bersch, M. A. Miri, G. Onishchukov, D. N. Christodoulides, and U. Peschel, Nature (London) **488**, 167 (2012).

[19] Y. J. Chen, A. W. Snyder, and D. N. Payne, IEEE J. Quantum Electron. **28**, 239 (1992).

[20] H. Ramezani, T. Kottos, R. El-Ganainy, and D. N. Christodoulides, Phys. Rev. A **82**, 043803 (2010).

[21] A. A. Sukhorukov, Z. Y. Xu, and Yu. S. Kivshar, Phys. Rev. A **82**, 043818 (2010).

[22] Z. H. Musslimani, K. G. Makris, R. El-Ganainy, and D. N. Christodoulides, Phys. Rev. Lett. **100**, 030402 (2008).

[23] S. V. Dmitriev, A. A. Sukhorukov, and Yu. S. Kivshar, Opt. Lett. **35**, 2976 (2010).

[24] S. M. Hu, X. K. Ma, D. Q. Lu, Z. J. Yang, Y. Z. Zheng, and W. Hu, Phys. Rev. A **84**, 043818 (2011).

[25] F. K. Abdullaev, Y. V. Kartashov, V. V. Konotop, and D. A. Zezyulin, Phys. Rev. A **83**, 041805 (2011).

[26] Z. W. Shi, X. J. Jiang, X. Zhu, and H. G. Li, Phys. Rev. A **84**, 053855 (2011).

[27] X. Zhu, H. Wang, L. X. Zheng, H. G. Li, and Y. J. He, Opt. Lett. **36**, 2680 (2011).

[28] D. A. Zezyulin, Y. V. Kartashov, and V. V. Konotop, Europhys. Lett. **96**, 64003 (2011).

[29] S. Nixon, L. J. Ge, and J. K. Yang, Phys. Rev. A **85**, 023822 (2012).

[30] S. M. Hu, X. K. Ma, D. Q. Lu, Y. Z. Zheng, and W. Hu, Phys. Rev. A **85**, 043826 (2012).

[31] D. A. Zezyulin and V. V. Konotop, Phys. Rev. A **85**, 043840 (2012).

[32] Y. J. He, X. Zhu, D. Mihalache, J. L. Liu, and Z. X. Chen, Opt. Commun. **285**, 3320 (2012).

[33] J. H. Zeng and Y. H. Lan, Phys. Rev. E **85**, 047601 (2012).

[34] S. V. Suchkov, B. A. Malomed, S. V. Dmitriev, and Yu. S. Kivshar, Phys. Rev. E **84**, 046609 (2011).

[35] R. Driben and B. A. Malomed, Opt. Lett. **36**, 4323 (2011).

[36] R. Driben and B. A. Malomed, Europhys. Lett. **96**, 51001 (2011).

[37] N. V. Alexeeva, I. V. Barashenkov, A. A. Sukhorukov, and Yu. S. Kivshar, Phys. Rev. A **85**, 063837 (2012).

[38] A. M. Kosevich and A. S. Kovalev, Zh. Éksp. Teor. Fiz. **67**, 1793 (1974) [JETP **67**, 891 (1975)]; R. F. Dashen, B. Hasslacher, and A. Neveu, Phys. Rev. D **11**, 3424 (1975); H. Segur and M. D. Kruskal, Phys. Rev. Lett. **58**, 747 (1987); J. P. Boyd, Nonlinearity **3**, 177 (1990).

[39] K. Li and P. G. Kevrekidis, Phys. Rev. E **83**, 066608 (2011).

[40] S. V. Dmitriev, S. V. Suchkov, A. A. Sukhorukov, and Yu. S. Kivshar, Phys. Rev. A **84**, 013833 (2011).

[41] A. Szameit, M. C. Rechtsman, O. Bahat-Treidel, and M. Segev, Phys. Rev. A **84**, 021806 (2011).

[42] S. V. Suchkov, S. V. Dmitriev, B. A. Malomed, and Yu. S. Kivshar, Phys. Rev. A **85**, 033825 (2012).

[43] Yu. S. Kivshar and G. P. Agrawal, *Optical Solitons: From Fibers to Photonic Crystals* (Academic Press, San Diego, 2003).

[44] T. Ueda and W. L. Kath, Phys. Rev. A **42**, 563 (1990).

[45] B. A. Malomed and S. Wabnitz, Opt. Lett. **16**, 1388 (1991).

[46] V. K. Mesentsev and S. K. Turitsyn, Opt. Lett. **17**, 1497 (1992).

[47] D. J. Kaup, B. A. Malomed, and R. S. Tasgal, Phys. Rev. E **48**, 3049 (1993).

[48] M. Haelterman and A. Sheppard, Phys. Rev. E **49**, 3376 (1994).

[49] M. Haelterman, A. P. Sheppard, and A. W. Snyder, Opt. Commun. **103**, 145 (1993).

[50] Y. Silberberg and Y. Barad, Opt. Lett. **20**, 246 (1995).

[51] J. Yang and D. J. Benney, Stud. Appl. Math. **96**, 111 (1996).

[52] J. K. Yang, Physica D **108**, 92 (1997).

[53] J. K. Yang, Stud. Appl. Math. **98**, 61 (1997).

[54] J. K. Yang, Phys. Rev. E **64**, 026607 (2001).

[55] Y. Tan and J. K. Yang, Phys. Rev. E **64**, 056616 (2001).

[56] R. Driben and B. A. Malomed, Europhys. Lett. **99**, 54001 (2012).

[57] N. N. Rosanov, *Spatial Hysteresis and Optical Patterns*, Springer Series in Synergetics (Springer, New York, 2002).

[58] *Dissipative Solitons*, edited by N. Akhmediev and A. Ankiewicz, Lecture Notes in Physics Vol. 661 (Springer, New York, 2005).

[59] N. V. Alexeeva, I. V. Barashenkov, and D. E. Pelinovsky, Nonlinearity **12**, 103 (1999); I. V. Barashenkov, N. V. Alexeeva, and E. V. Zemlyanaya, Phys. Rev. Lett. **89**, 104101 (2002); I. V. Barashenkov, E. V. Zemlyanaya, and T. C. van Heerden, Phys. Rev. E **83**, 056609 (2011).